EXPERIMENTAL STUDY ON VORTEX RINGS DYNAMICS IN A PULSED JET USING PARTICLE IMAGE VELOCIMETRY

Massimo Falchi
Department of Mechanics and Aeronautics,
University of Rome "La Sapienza"
Via Eudossiana 18, 00184 Rome – Italy
E-mail: massimo.falchi@uniroma1.it

Giovanni Paolo Romano
Department of Mechanics and Aeronautics,
University of Rome "La Sapienza"
Via Eudossiana 18, 00184 Rome – Italy
E-mail: romano@dma.ing.uniroma1.it

ABSTRACT

In this work, an experimental study on vortex rings dynamics has been performed using digital particle image velocimetry (PIV); in particular, vortex rings at the exit of a circular orifice in a pulsed jet configuration are investigated. The relevance of such a study is related both to the fundamental fluid-mechanics involved in the generation, growing and evolution of vortex rings and simultaneously to the practical applications of the pulsed jet configuration; in particular attention is given to the pulsed jet condition which appears at the outlet of prosthetic heart valves.
Different input signals and different stroke volumes have been studied obtaining great differences in the fluid dynamic fields, in particular in the number and in the dynamics of the generated vortices; Reynolds and viscous stresses calculations have been performed.
For this particular experimental set-up, results show a great dependency from the input signal imposed at the piston by the linear motor used, both in the waveform, and in stroke volume.

INTRODUCTION

Due to its great importance in very different fields, vortex rings dynamics is one of the most studied topic in fluid mechanics; from volcanos eruptions to the blood discharge in the aortic vessel, vortex rings play a central role and can be identified as the main important feature. For these reasons, great efforts have been done in the past and still more will be spent in the future; in fact despite of all the work devoted to it still more has to be understood. In recent years many valuable different studies have been published devoted to this topic; the review of Shariff (1992), the work of Gharib (1998) among the others have shown how little it is known about them. Vortex rings have been studied using different approaches: visualizations were the first attempt to have a more deep insight in the phenomenom, then optical measurements came up giving much more results. In addition to that, vortex rings can be produced in many different ways each of them being valuable of attention; producing vortex rings pushing water through a nozzle with an angle is the most common way. Also the use of an orifice in a plate is a very common way togheter with the use of a circular cylinder in which a piston can push the water or some other fluid in it giving the so called slug-flow model. Basically all the results available in the literature regard these types of producing vortex rings; in the present study a different method is used. This different experimental set-up has been thought to better capture the characteristics of the blood flow from the left atrium to the ventricular cavity of the human heart. To this aim, a careful design of the mechanical device which drives the piston generating the vortex ring has been performed. This is a very important point for stating the suitability of a given mock-loop for testing among different prosthetic heart valves. The aim of the paper is to investigate the effect of different driving signals for the piston and of the flow rate on the intensity, shape and evolution of the generated vortex rings.

EXPERIMENTAL SETUP

The experimental apparatus, represented in Figure n 1, involved in the experiments consists of a feeding tank W (equipped with two gravity one-way valves V_1 and V_2) connected to a transparent test tank S (size 110×40×40 cm respectively along streamwise direction x and transverse directions y and z) through inlet and outlet pipes. During the backward motion of the piston (which is the driving system for the flow field), water flows into the test tank along the inlet pipe. During forward motion of the piston, a honeycomb (5 cm thickness) is used to smooth velocity fluctuations and large scale vortices; at about 30 cm from the honeycomb S_n , a circular orifice (diameter D_0=3 cm) on a transverse plane S_1 generates an axi-symmetric jet which flows into the proper test section. This is the section in which the jet flows almost freely and the velocity field is measured with the PIV system on (x,y) and (y,z) planes; the motivation to use an orifice section to generate the jet resides in minimising the effects on the field due to boundary conditions. Through a large hole (diameter equal to 15 cm in a plate S_2), the flow goes into the discharge section; this avoids disturbances from the outlet section to propagate upstream. Water flows to the feeding tank through the outlet pipe. The test section is equipped at the top with valves which allow air to be eliminated. Artificial seeding has been not used due to the presence of natural small density seeding in the flowing water.

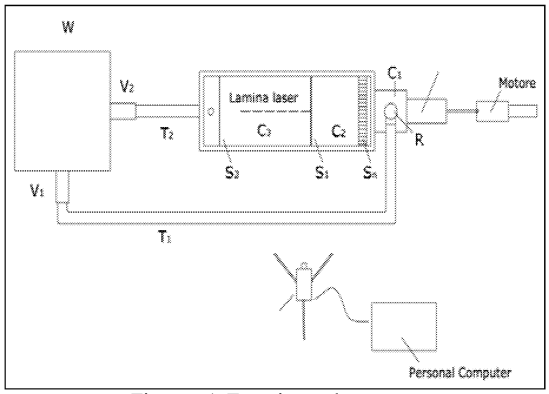

Figure n 1: Experimental apparatus.

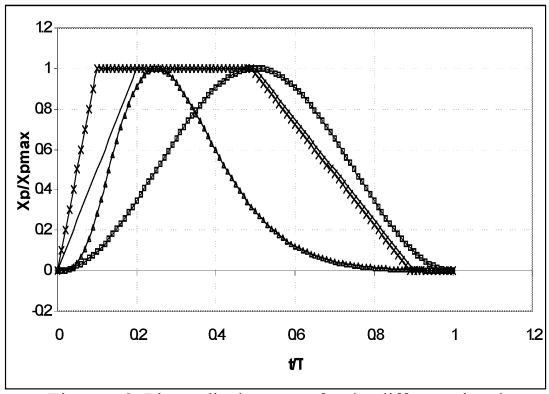

Figure n 2: Piston displacement for the different signals.

The pulse used to start the vortex ring is generated by a cylindrical piston (diameter D_p=10 cm) driven by a 500W synchronous linear motor (*brashless cog-free*). A control software provides the signal *i.e.* the displacement in time to be executed by the motor; it is possible to change independently frequency, amplitude and shape of the signal (up to 1000 points in a cycle). A digital optical encoder ensures the control of the effective piston position in time allowing a feedback correction of the imposed displacement; the actual and initial positions of the piston are compared and an incremental error is computed to correct drift (error in position less than 0.5%). A trigger signal is provided at the beginning of each cycle to start phase-sampling of PIV images; an advanced commercial PIV system (by LaVision) is used to acquire and analyse the images. The spatial resolution of the acquired images is equal to 1/0.0754 mm^{-1} (the orifice diameter D_0=3 cm corresponds to 398 pixel), while the time resolution is equal to 1/0.00035 s^{-1} (time interval between image pairs equal to 350 μs). The number of PIV images acquired at each phases is equal to 50 (a detailed statistical analysis of the effect on the results of averaging over 10, 50 100 or 1000 images has been also performed indicating that 50 can get affordable average fields in terms of velocity vector and vorticity).

In connection to prosthetic heart valve testing, the following signals in time have been considered (refer to Figure n. 2 in which the displacements of the piston in time are given):

- sinusoidal oscillation (sinusoidal);
- trapezoidal signal with fast ramp (ramp1);
- trapezoidal signal with slow ramp (ramp2);
- exponential decay, defined as $x(t) = t^4 e^{(1-t)}$ (exponential).

Table n 1: Characteristic parameter of the studied signals.

Signal	V(ml)	L_p(cm)	L_p/D_p	$(U_p)_m$ (cm/s)	U_pD_p/v	L_p/D_0
sinus	50	0.64	0.21	1.28	1280	2.35
sinus	70	0.89	0.30	1.78	1780	3.30
sinus	90	1.15	0.38	2.30	2300	4.23
exp	50	0.64	0.21	2.56	2560	2.35
exp	70	0.89	0.30	3.56	3560	3.30
exp	90	1.15	0.38	4.60	4600	4.23
ramp1	70	0.89	0.30	8.90	8900	3.30
ramp2	70	0.89	0.30	4.45	4450	3.30

In Table n 1 the characteristic parameters for each signal studied are reported with V stroke volume, L_p piston run length, D_p piston diameter, $(U_p)_m$ piston average velocity, D_0 orifice diameter, L_p/D_0 formation number according to Gharib (1998). For each of them, the tested flow rate was 70 ml; for the sinusoidal and the exponential signals 50 and 90 ml have been also investigated and compared (these values are typical of physiological conditions). Following Gharib (1998), the formation number, *i.e.* the number at which the leading vortex separates from the other vortices, at the orifice section has been calculated for the three stroke volume and are reported in Table n. 1 (last column).
The frequency of the signals was always fixed at 1 Hz (typical human beat frequency).

RESULTS

Various results will be presented in the following sections. First of all a characterization of the hydraulic circuit will be given in terms of velocity profiles at the orifice exit section in particular for the sinusoidal and the exponential signals. Then vorticity data, in terms of vorticity fields will be shown in the next section. A comparison beetwen the four different signals at the stroke volume of 70 ml will be presented followed by a comparison beetwen different stroke volume - 50, 70 and 90 ml - for the sinusoidal and the exponential signals. Then a comparison of viscous and Reynolds stresses will be shown for the sinusoidal and the exponential signals.

Velocity profiles

For all the acquired data, velocity profiles at the outlet of the orifice have been extracted and plotted for the various signals at the different time phases and flow rates in order to understand the effects of these parameters . The behaviour in time of the flow rate (or equivalently of the average flow velocity) at the outlet of the orifice can be evaluated and compared with the velocity derived from the rigid piston displacement given in Figure 1. This comparison is given in Figure 3 and 4 for the sinusoidal and exponential signals for three values of the nominal flow rate. The data collapse very well both in the discharge (positive velocities) and in the regurgitation parts (negative velocities); it must be noticed that in the exponential signal there is no delay between the driving signal and the measured one, while for the sinusoidal there is almost a quarter of cycle delay between the two. This does mean that the hydraulic circuit (*i.e.* the simulation of the blood circulation system) may react differently to different pulse shapes.

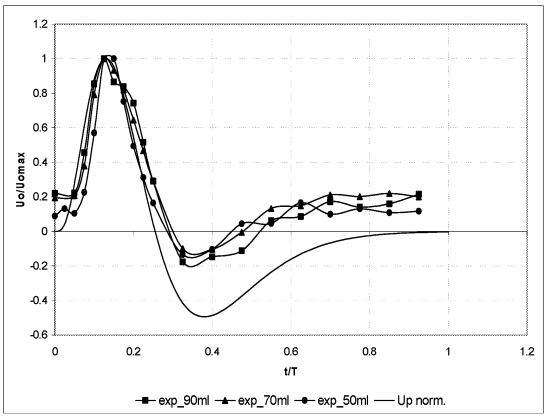

Figure 3: Velocity profiles for sinusoidal signal

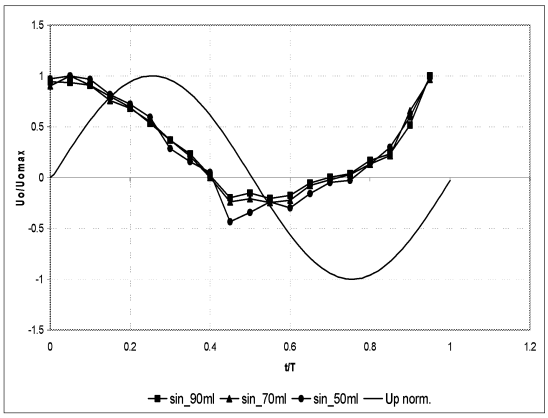

Figure 4: Velocity profiles for exponential signal

Vorticity fields

In this section vorticity fields are reported giving particular attention to the differences in the vortices structure, position and interactions for the various conditions studied.

The sinusoidal signal, for different values of the stroke volume, is depicted in Figure 4 at a phase position of $\Delta t/T=0.15$. As it is possible to observe, it can be noticed that the vortex ring reaches larger distances from the orifice as high the volume rate; consequently, the flow velocity are also higher. On the other hand, the flow configuration seems to be quite similar between the different conditions thus allowing a sort of independence on the flow volume rate, and of the formation number. This characteristic matches well with the results shown in the previous section containing the results in terms of velocity profiles at the inlet which didn't vary with the stroke volume. It has to be noticed that even in the case of stroke volume equal to 50 ml - formation number equal to 2.35 - the leading vortex ring is followed by some secondary vortex rings that tends to merge forming the so-called trailing jet. Obviously the intensity of the leading vortex ring increases with the stroke volumes as a consequence of an increment of the total circulation flux through the orifice. It also should be noticed that the leading vortex interacts with the trailing jet with a sort of bridge (see b)).

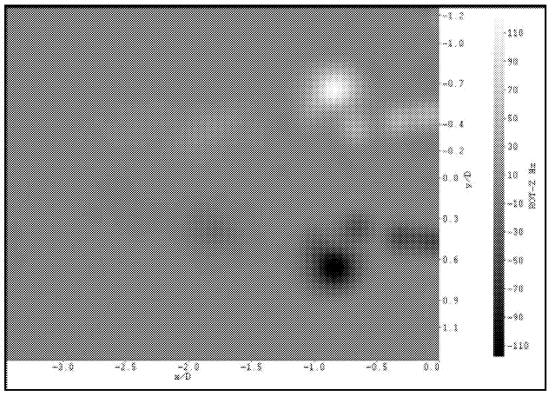
a)

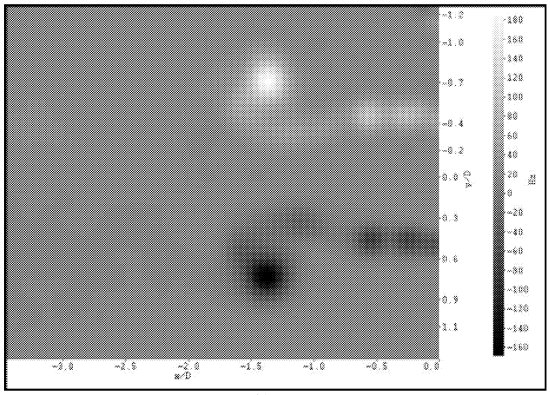
b)

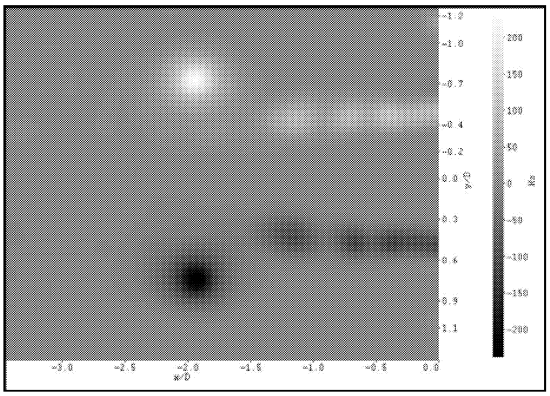
c)

Figure 4: Mean vorticity plots (average over 50 images). Sinusoidal signal at phase $\Delta t/T=0.15$. Displaced flow volume equal to a) 50 ml (at the top left), b) 70 ml (at the top right) and c) 90 ml (at the bottom). Flow from right to left.

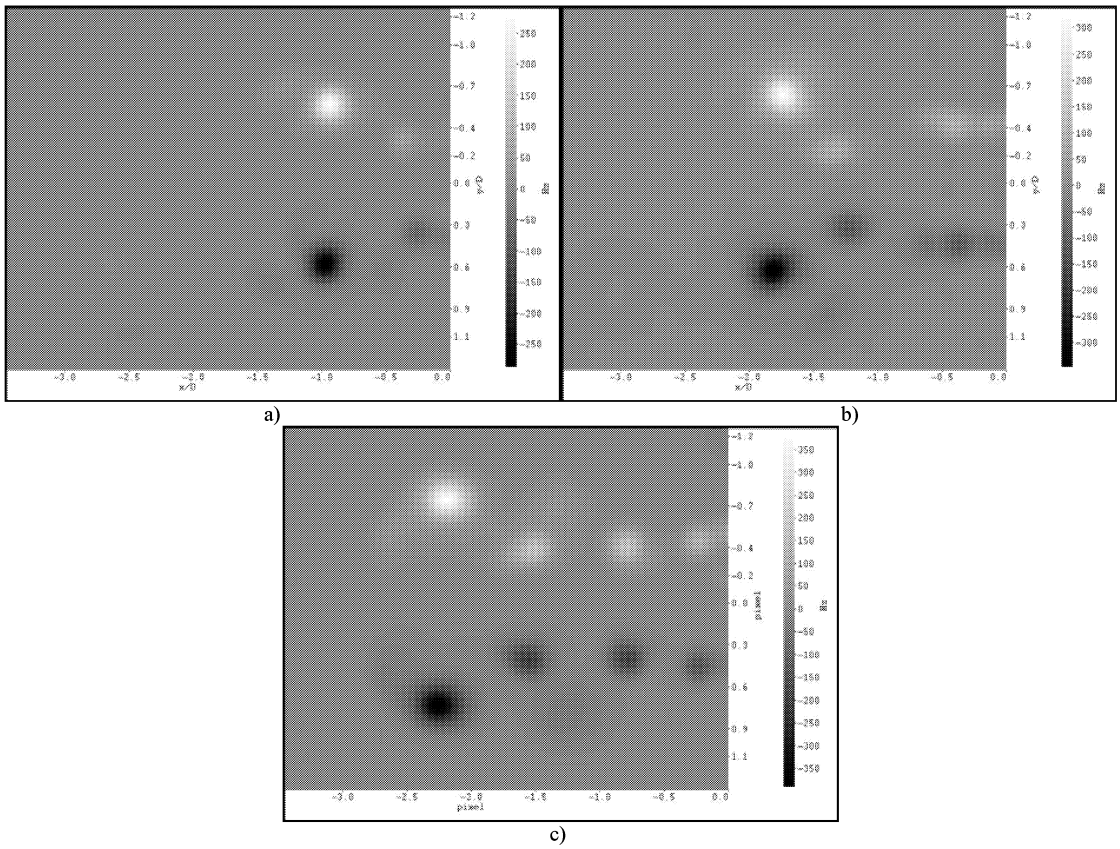

Figure 4: Mean vorticity plots (average over 50 images). Exponential signal at phase Δt/T=0.25. Displaced flow volume equal to a) 50 ml (at the top left), b) 70 ml (at the top right) and c) 90 ml (at the bottom). Flow from right to left.

Similar results are obtained for the exponential signal, Figure 4; in this case, there are some differences in the intensity of the secondary vortices in the wake (which now are much more point-like in comparison to the distributed wake of the sinusoidal case). They attain higher intensities for larger volume rate, while the configurations and the intensities of the primary vortex ring are very similar for the different volume rates. It is interesting to note that both for the sinusoidal and exponential signal, the separation between the vortices increases with the volume rate; this is not predicted by theories which give constant separation. The comparison between sinusoidal and exponential reveals that the structure of the trailing jet in the wake and the interaction between this and the vortex ring are different. In particular, for the exponential signal there is a stronger deformation of the vortical wake due to the interaction with the leading vortex ring; this interaction causes the roll-up of the closest vortex in the wake around the primary vortex ring (this phenomenon is known as leapfrogging in the literature on the argument).

In Figure 5, the flow phase averaged fields obtained with the four signals are compared (on a (x,y) plane, at a non-dimensional phase in time $\Delta t/T$=0.2 which corresponds to well established vortex rings for all conditions). The velocity values for the exponential and the ramp2 signals are larger that that for the sinusoidal (but the vortex ring position is more or less the same between these three cases). For the ramp1 signal (the fastest one, see Figure 2), the velocities are largely higher and the vortex ring moved further downstream in comparison to the other signals. This fact is responsible for the different interactions with the vortex ring wake; in the case of the sinusoidal signal, the trailing jet wake is quite regular and aligned with the orifice. For the exponential and ramp2 signals, the primary vortex rings are closer between them and this causes a deformation of the wake in the form of inclined vortices for the exponential case and of more concentrated (point-like) vortices for the ramp2. In the case of the ramp1, the roll-up of the wake into the primary vortex ring leads to a condition in which wake vortices almost disappear being convected with the primary one (and rotating around it). This means that as quicker the forward run of the piston (*i.e.* as faster the driving signal) as lower the intensity of the trailing jet wake. To summarize, the following phenomena have been recognised:

- absence of interaction between primary and trailing vortices (which appears in the form of an almost continuous layer) for the sinusoidal case;
- interaction and simultaneous deformation of the wake (in the form of point-like vortices) for the cases of exponential and ramp2 signals;
- strong roll-up of the wake into the field of the primary vortex and almost vanishing remaining wake for the case of the ramp1 signal.

In particular, the last phenomenon is connected to a residual vorticity (outside the ring) after the vortex ring generation which doesn't move from locations close to the orifice during the regurgitation phase (backward motion of the piston). This vorticity interacts with the next generated vortex ring giving rise to complex phenomena.

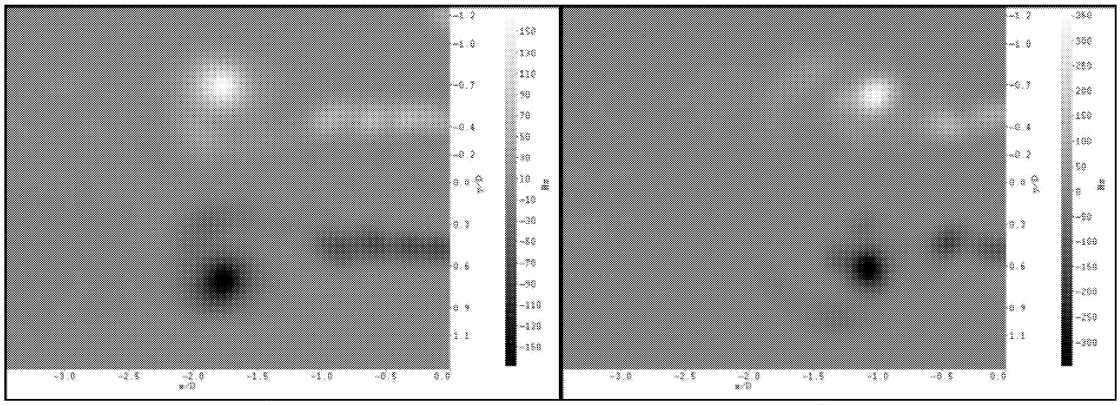

a) b)

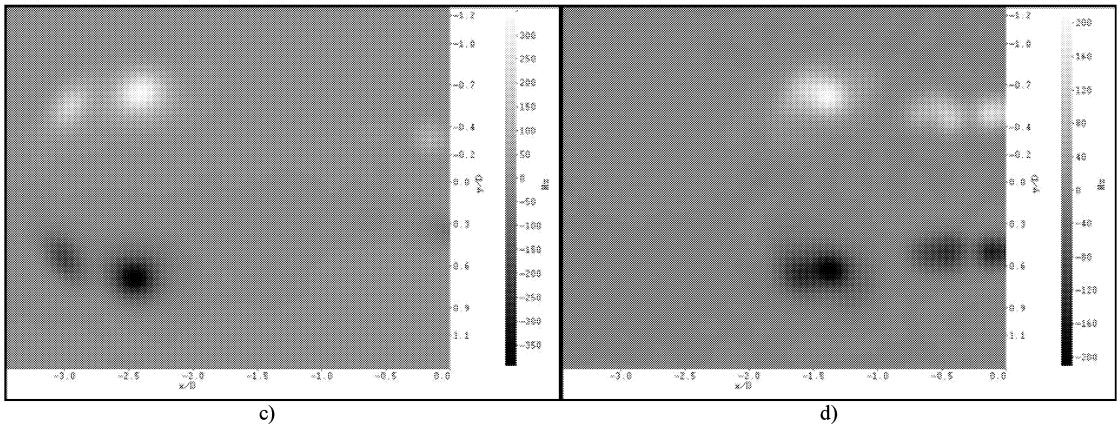

c) d)

Figure 5: Mean vorticity plots (average over 50 images). Comparison between a) sinusoidal (at the top left), b) exponential (at the top right), c) ramp1 (at the bottom left) and d) ramp2 (at the bottom right) at phase $\Delta t/T=0.2$. Displaced flow volume equal to 70 ml.

In Figure 6 particular attention is given to the fast ramp signal - ramp 1. For two time delays, vorticity plots are presented. The main characteristics have already been described but it is important to note the particular behaviour of the vortex cores interactions. In fact it is possible to observe a very fascinating phenomenom; in a) two pairs of vortices are merging, followed by another pair. In b) these vortices are overtaking the leading vortex which has already merged with a secondary vortex - and this can be seen by the strecthed vortex form -. For this particular signal the leapfrogging seems to involve more than two vortex cores.

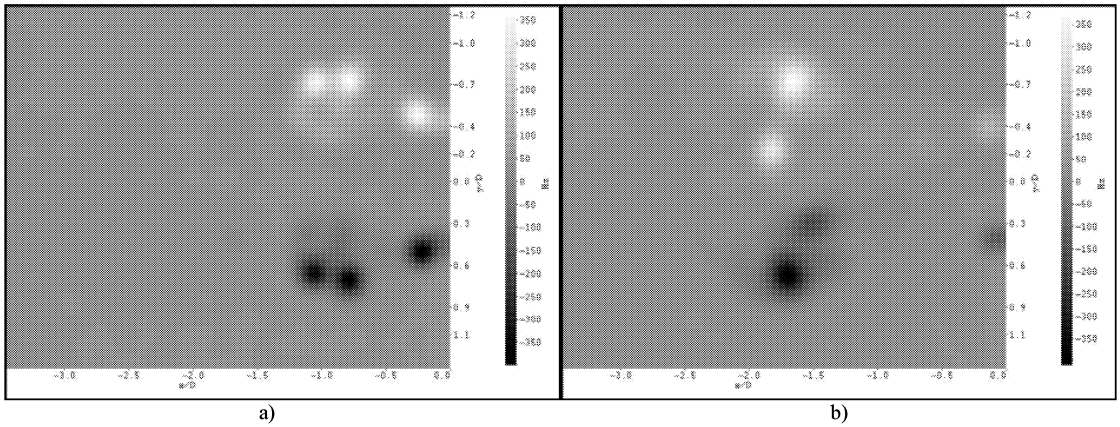

a) b)

Figure 6: Mean vorticity plots (average over 50 images) for the ramp1 signal at two different time delays. a) $\Delta t/T= 0.1$, b) $\Delta t/T= 0.15$ Displaced flow volume equal to 70 ml.

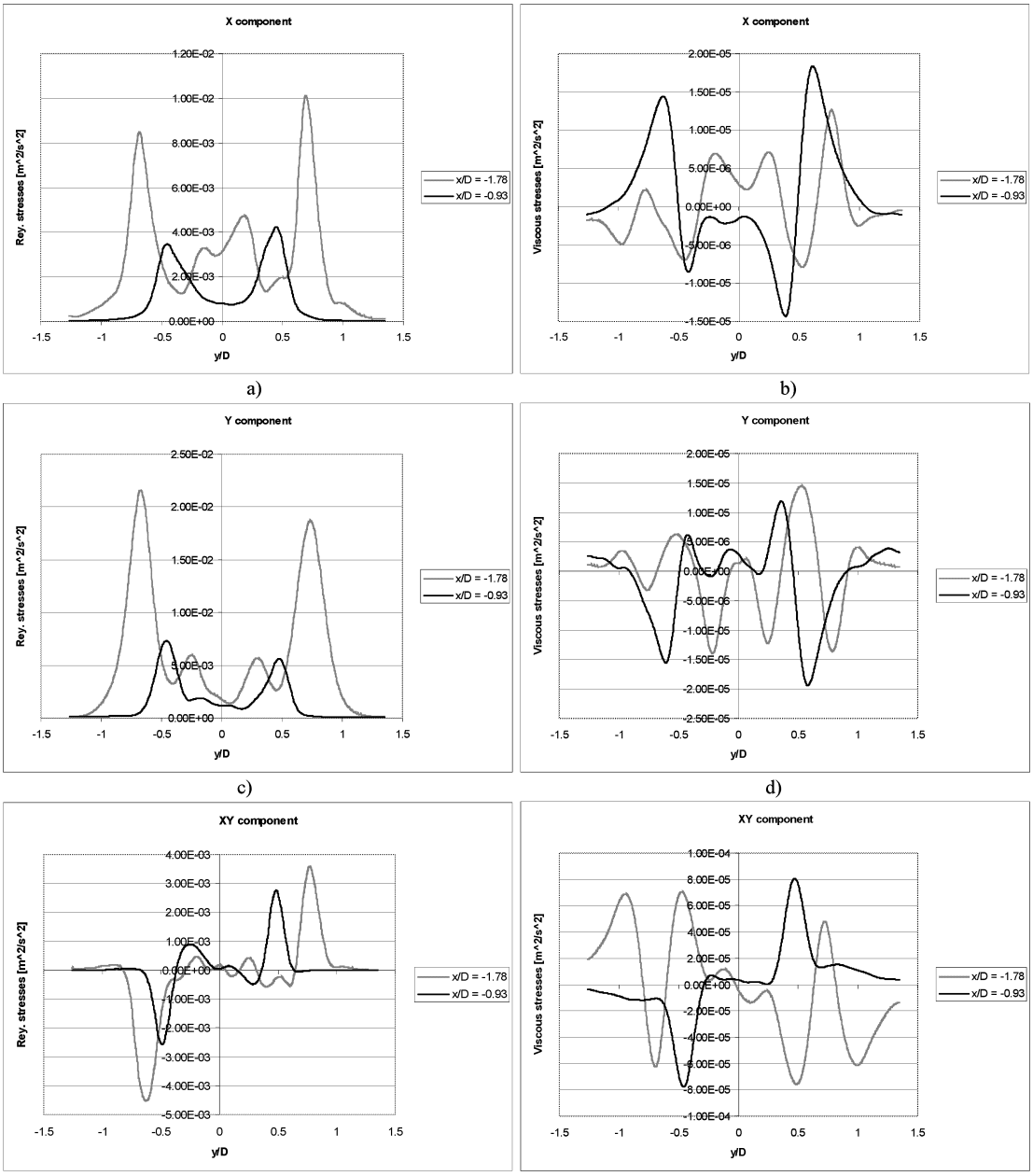

Figure 7: Stresses fields for the sinusoidal signal at $\Delta t/T = 0.2$. a) XX Reynolds stress component, b) XX Viscous stress component, c) YY Reynolds stress component, d) YY Viscous stress component, e) XY Reynolds stress component, f) XY Viscous stress component. Displaced flow volume equal to 70 ml.

Stresses profiles

In Figure 7 Reynolds and viscous stresses are presented; due to the Reynolds number involved - see Table n 1 - viscous stresses are negligible in respect to Reynolds ones - more than two orders of magnitude higher. In addition to that it has to be noted that the three component has more or less the same intensity. On the contrary Reynolds stresses show different values; the YY component is two times the XX one and three times the XY one. It also has to be noted that Reynolds stresses at the second station (x/D = -1.78) are larger than those at the first one (x/D = -0.93) while an opposite situation stands for the viscous ones.

Acknowledgements

The Authors wish to thank LAVISION GmbH and in particular Dr. Bernhardt Wieneke. The work has been performed under financial support by European Community (IST 2002, 37548 Smart-Piv Project).

References

Gharib, M., Rambod, E. and Shariff, K., 1998, "A Universal Time Scale for Vortex Ring Formation", *Journal of Fluid Mechanics*, Vol. 360, pp. 121 – 140.

Shariff, K and Leonard, A., 1992, "Vortex Rings", *Annual Review of Fluid Mechanics*, Vol. 24, pp. 235 - 279